

Cosmological Constraints on the Modified Entropic Force Model

Hao Wei*

Department of Physics, Beijing Institute of Technology, Beijing 100081, China

ABSTRACT

Very recently, Verlinde considered a theory in which space is emergent through a holographic scenario, and proposed that gravity can be explained as an entropic force caused by changes in the information associated with the positions of material bodies. Then, motivated by the Debye model in thermodynamics which is very successful in very low temperatures, Gao modified the entropic force scenario. The modified entropic force (MEF) model is in fact a modified gravity model, and the universe can be accelerated without dark energy. In the present work, we consider the cosmological constraints on the MEF model, and successfully constrain the model parameters to a narrow range. We also discuss many other issues of the MEF model. In particular, we clearly reveal the implicit root to accelerate the universe in the MEF model.

PACS numbers: 98.80.Es, 95.36.+x, 04.50.-h, 04.50.Kd

* email address: haowei@bit.edu.cn

I. INTRODUCTION

Very recently, Verlinde [1] considered a theory in which space is emergent through a holographic scenario, and proposed that gravity can be explained as an entropic force caused by changes in the information associated with the positions of material bodies. In this scenario, Verlinde has successfully derived the Newton's law of gravitation, the Einstein equations, and the law of inertia, from the entropic point of view. In fact, the entropic force scenario is similar to the old idea of Jacobson [2], but also beyond it in some sense. Similar entropic insight into gravity has also been made by Padmanabhan [3] independently and simultaneously.

Here we briefly mention some key points of the entropic force scenario following [1]. Motivated by Bekenstein's argument [4], Verlinde postulated that the change in entropy near the holographic screen is linear in the displacement Δx , namely,

$$\Delta S = 2\pi k_B \frac{mc}{\hbar} \Delta x, \quad (1)$$

where m is the mass of test particle, whereas k_B , c and \hbar are Boltzmann constant, speed of light and the reduced Planck constant, respectively. The effective entropic force acting on the test particle due to the change in entropy obeys the first law of thermodynamics

$$F \Delta x = T \Delta S, \quad (2)$$

where T is the temperature. If one takes the Unruh temperature T experienced by an observer in an accelerated frame whose acceleration is a , i.e.,

$$k_B T = \frac{1}{2\pi} \frac{\hbar a}{c}, \quad (3)$$

to be the temperature associated with the bits on the holographic screen, from Eqs. (1)–(3), it is easy to recover the second law of Newton

$$F = ma. \quad (4)$$

Considering a sphere as the holographic screen, Verlinde assumed that the number of used bits on the holographic screen N is proportional to the area $A = 4\pi r^2$, i.e.,

$$N = \frac{Ac^3}{G\hbar}. \quad (5)$$

According to the equipartition law of energy, the total energy inside the screen is

$$E = \frac{1}{2} N k_B T. \quad (6)$$

Of course, one can identifies E with the mass M inside the screen through

$$E = Mc^2. \quad (7)$$

From Eqs. (1), (2), and (5)–(7), one can recover the Newton's law of gravitation

$$F = G \frac{Mm}{r^2}, \quad (8)$$

where G can be identified with the Newton constant now. From Eqs. (3), (4) and (8), it is easy to find the gravitational acceleration

$$g = \frac{GM}{r^2}, \quad (9)$$

and the temperature

$$T = \frac{\hbar}{k_B c} \frac{g}{2\pi}. \quad (10)$$

As shown in [1], a relativistic generalization of the presented arguments directly leads to the Einstein equations. We strongly refer to the original paper [1] for great details.

Soon after Verlinde's proposal of entropic force, many relevant works appeared. For examples, Cai, Cao and Ohta [5], Shu and Gong [6] derived the Friedmann equations from entropic force simultaneously. Smolin [7] derived the Newtonian gravity in loop quantum gravity. Li and Wang [8] showed that the holographic dark energy can arise in the entropic force scenario. Easson, Frampton and Smoot [9] considered the entropic accelerating universe and the entropic inflation. Tian and Wu [10], Myung [11] discussed the thermodynamics of black holes in the entropic force scenario. Vancea and Santos [12] considered the uncertainty principle from the point of view of entropic force. Zhang, Gong and Zhu [13], Sheykhi [14] derived the modified Friedmann equation from the corrected entropy. Also, Modesto and Randono [15] discussed the corrections to Newton's law from the corrected entropy. Cai, Liu and Li [16] considered a unified model of inflation and late-time acceleration in the entropic force scenario. For other relevant works to entropic force, we refer to e.g. [17–19, 36] and references therein.

The works mentioned above are in fact closely following Verlinde's proposal of entropic force [1]. To be honest, here we should also mention the other works which are strongly criticizing the entropic force scenario. For instance, the author of [38] argued that there are some possible flaws in Verlinde's idea. In [39], Culetu argued that the relativistic Unruh temperature cannot be associated with the bits on the screen in the form considered by Verlinde. In [40], Hossenfelder argued that some additional assumptions made by Verlinde are unnecessary and there are some gaps in Verlinde's arguments. In [41], Myung found that entropic force does not always imply the Newtonian force law, and the connection between Newtonian cosmology and entropic force cannot be confirmed. In [42], Li and Pang found that inflation is inconsistent with the entropic force scenario. In [43], Lee argued that there are some inconsistencies in Verlinde's arguments from a classical point of view.

So far, we have briefly surveyed the current status of the works relevant to the entropic force scenario. It is fair to say that the entropic force scenario is still in controversy. On the other hand, there is no breakthrough on entropic force after Verlinde's proposal [1]. A deep insight is needed to understand the nature of gravity. In addition, further discussions on the entropic force scenario are also desirable. Only when more and more results on entropic force are available, one can say something conclusively at that time. To this end, we would like to contribute our effort and try to learn more about the entropic force scenario. In this work, we will consider a modified entropic force scenario proposed by Gao [20], which has some interesting features. And then, we will constrain the modified entropic force scenario with the latest observational data.

In [20], Gao noted that statistical thermodynamics reveals the equipartition law of energy does not hold in the very low temperatures. Instead, as is well known, the Debye model [21, 22] is very successful in explaining the experimental results when the temperatures are very low. Since the equipartition law of energy plays an important role in the derivation of entropic force, the entropic force should be modified for the very weak gravitational fields which correspond to very low temperatures. Especially, the large-scale universe is in such an extreme weak gravitational field, and hence the modified entropic force (MEF) makes sense in cosmology.

Following [20], we briefly mention the key points of MEF model. Similar to the Debye model [21, 22] in thermodynamics, one can modify the equipartition law of energy in Eq. (6) to

$$E = \frac{1}{2} N k_B T D(x), \quad (11)$$

where $D(x)$ is the Debye function which is defined by

$$D(x) = \frac{3}{x^3} \int_0^x \frac{y^3}{e^y - 1} dy, \quad (12)$$

and x is related to the temperature T as

$$x \equiv \frac{T_D}{T}, \quad (13)$$

in which T_D is the Debye temperature. By definition, x is positive. With the modified equipartition law of energy, namely Eq. (11), similar to the original entropic force, one can easily obtain [20]

$$g = \frac{GM}{r^2} \frac{1}{D(x)}, \quad (14)$$

in which (nb. Eq. (10))

$$x = \frac{T_D}{T} = \frac{g_D}{g}, \quad (15)$$

where $g_D \equiv (2\pi k_B c/\hbar) T_D$ is the Debye acceleration. Actually, Eq. (14) corresponds to the modified Newtonian law of gravity. In the limit of strong gravitational field, $g \gg g_D$ and hence $x \ll 1$, from Eq. (12) it is easy to find that $D(x) \rightarrow 1$ and the Newtonian gravity is recovered. On the other hand, in the limit of weak gravitational field, $g \ll g_D$ and hence $x \gg 1$, one can see that $D(x) \rightarrow \pi^4/(5x^3)$ and then $g \propto 1/\sqrt{r}$, which significantly deviates from the familiar inverse square law [20]. However, as argued in [20], one need not to worry about the possibility of MEF against the experimental results of the inverse square law. Since these experiments testing the inverse square law were done on the Earth or in the solar system, which are actually in the strong gravitational fields, we have $x \ll 1$ and $D(x) \rightarrow 1$, therefore the deviation from the inverse square law are extremely tiny. The significant deviation from the inverse square law can only occur in the very large scale in the universe where the gravitational fields are very weak, and hence it can escape the detection of these experiments testing the inverse square law. Of course, this argument relies on a small g_D . We will justify it later in the present work.

Next, we turn to the cosmological issues in the MEF Model. For convenience, we set the units $k_B = c = \hbar = 1$ hereafter. Using the derivation method in [5, 6], one can find that the modified Raychaudhuri equation is given by [20]

$$4\pi G(\rho + p) = -\left(\dot{H} - \frac{K}{a^2}\right) \left[-2D(x) + \frac{3x}{e^x - 1}\right], \quad (16)$$

where ρ and p are the total energy density and total pressure of cosmic fluids, respectively; K is the spatial curvature of the universe; $H \equiv \dot{a}/a$ is the Hubble parameter; $a = (1+z)^{-1}$ is the scale factor (we have set $a_0 = 1$); z is the redshift; a dot denotes the derivatives with respect to cosmic time t ; the subscript “0” indicates the present value of the corresponding quantity. Taking into account the Hawking temperature T for the universe [23]

$$T = \frac{H}{2\pi}, \quad (17)$$

from Eqs. (13) and (15), it is easy to see that

$$x = \frac{H_D}{H}, \quad (18)$$

where $H_D = g_D$. On the other hand, the energy conservation equation still holds in the MEF model, namely

$$\dot{\rho} + 3H(\rho + p) = 0. \quad (19)$$

From Eqs. (16) and (19), one can derive the corresponding Friedmann equation. It is anticipated that Friedmann equation is also modified, $H^2 \neq (8\pi G\rho)/3$, due to the correction term $-2D(x) + 3x/(e^x - 1)$ in Eq. (16). The MEF model is in fact a modified gravity model. Gao showed that the MEF model can describe the accelerating universe without dark energy. We refer to the original paper [20] for details.

Since Gao has not considered the constraints on the MEF model in [20], we will try to obtain the cosmological constraints with the latest observational data in the next section. Further, we will discuss some relevant issues of the MEF model in Sec. III. Finally, we give the brief conclusion and some meaningful remarks in Sec. IV.

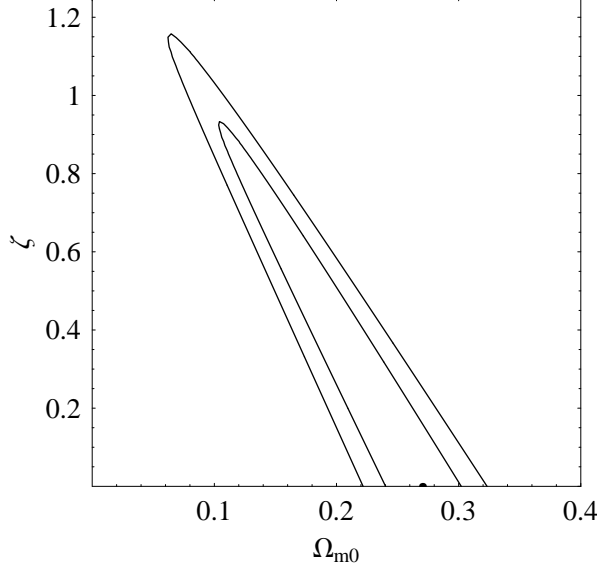


FIG. 1: The 68.3% and 95.4% confidence level contours in the $\Omega_{m0} - \zeta$ parameter space. The best-fit parameters are also indicated by a black solid point. This result is obtained by using the data of 557 Union2 SNIa alone.

II. COSMOLOGICAL CONSTRAINTS ON THE MEF MODEL

In this section, we consider the cosmological constraints on the MEF model. To this end, we firstly rewrite the equations to suitable forms. Notice that we consider a spatially flat universe (namely $K = 0$) throughout this work. From Eqs. (16) and (19), we have

$$8\pi G d\rho = 3 \left[-2D(x) + \frac{3x}{e^x - 1} \right] dH^2. \quad (20)$$

As in [20], we consider the universe contains only pressureless matter. So, we have $\rho = \rho_m = \rho_{m0} a^{-3} = \rho_{m0} (1+z)^3$. Dividing $3H_0^2$ in both sides of Eq. (20), we obtain

$$\Omega_{m0} da^{-3} = \left[-2D(x) + \frac{3x}{e^x - 1} \right] dE^2, \quad (21)$$

where

$$\Omega_{m0} \equiv \frac{8\pi G \rho_{m0}}{3H_0^2}, \quad E \equiv \frac{H}{H_0} = \frac{\zeta}{x}, \quad \zeta \equiv \frac{H_D}{H_0}. \quad (22)$$

Note that $\Omega_{m0} \neq \rho_{m0}/\rho_0 = 1$, because Friedmann equation has been modified in the MEF model, i.e., $H^2 \neq 8\pi G\rho/3$. By definition, ζ is positive. Finally, we get the differential equation for $E(z)$, namely

$$\left[-2D\left(\frac{\zeta}{E}\right) + \frac{3\zeta/E}{e^{\zeta/E} - 1} \right] \cdot 2E \frac{dE}{dz} = 3\Omega_{m0} (1+z)^2. \quad (23)$$

In principle, one can numerically find $E(z)$ from this exact differential equation, and then fit it to the observational data to get the constraints on the MEF model. However, we find that it consumes a large amount of time beyond normal patience when we scan the grid points in the parameter space, mainly due to the hardness of numerically solving the exact differential equation (23) in which $D(\zeta/E)$ is an integral whose upper limit is ζ/E itself. Therefore, it is advisable to find a reliable approximation of the

exact differential equation (23). Note that

$$-2D(x) + \frac{3x}{e^x - 1} = 1 - \frac{3}{4}x + \mathcal{O}(x^2), \quad (24)$$

for any small quantity x . On the other hand, in [20] one might find the hint of a small ζ (notice that it has been chosen to be 10^{-5} in [20] for example). Together with the well-known fact that usually $E(z)$ increases rapidly when z increases, ζ/E is a small quantity in Eq. (23). Therefore, we find that an approximation of the exact differential equation (23) is given by

$$\left(1 - \frac{3}{4}\frac{\zeta}{E}\right) \cdot 2E dE = \Omega_{m0} da^{-3}. \quad (25)$$

Integrating Eq. (25), we have

$$E^2 - \frac{3}{2}\zeta E = \Omega_{m0} a^{-3} + \text{const.}, \quad (26)$$

where *const.* is the integral constant, which can be determined by requiring $E(z=0) = 1$. Finally, we find that

$$E^2 - \frac{3}{2}\zeta E = \Omega_{m0} (1+z)^3 + \left(1 - \frac{3}{2}\zeta - \Omega_{m0}\right), \quad (27)$$

which is a quadratic equation of E in fact. Noting that E is positive, we solve Eq. (27) to get

$$E(z) = \frac{3}{4}\zeta + \frac{1}{2} \left\{ \frac{9}{4}\zeta^2 + 4 \left[\Omega_{m0} (1+z)^3 + \left(1 - \frac{3}{2}\zeta - \Omega_{m0}\right) \right] \right\}^{1/2}. \quad (28)$$

Obviously, when $\zeta \ll 1$, we see that the MEF model reduces to the familiar Λ CDM model in which $E(z) = [\Omega_{m0} (1+z)^3 + (1 - \Omega_{m0})]^{1/2}$. Therefore, it is not surprising that in [20] Gao found the MEF model with $\zeta = 10^{-5}$ is degenerate to Λ CDM model. In fact, this observation is indeed the key point to understand the reason for accelerating the universe without dark energy in the MEF model.

In the following, we consider the cosmological constraints on the MEF model from observational data. At first, we use the observational data of Type Ia supernovae (SNIa) alone. Recently, the Supernova Cosmology Project (SCP) collaboration released their Union2 compilation which consists of 557 SNIa [24]. The Union2 compilation is the largest published and spectroscopically confirmed SNIa sample to date. The data points of the 557 Union2 SNIa compiled in [24] are given in terms of the distance modulus $\mu_{obs}(z_i)$. On the other hand, the theoretical distance modulus is defined as

$$\mu_{th}(z_i) \equiv 5 \log_{10} D_L(z_i) + \mu_0, \quad (29)$$

where $\mu_0 \equiv 42.38 - 5 \log_{10} h$ and h is the Hubble constant H_0 in units of 100 km/s/Mpc, whereas

$$D_L(z) = (1+z) \int_0^z \frac{d\tilde{z}}{E(\tilde{z}; \mathbf{p})}, \quad (30)$$

in which \mathbf{p} denotes the model parameters. The χ^2 from 557 Union2 SNIa is given by

$$\chi_\mu^2(\mathbf{p}) = \sum_i \frac{[\mu_{obs}(z_i) - \mu_{th}(z_i)]^2}{\sigma^2(z_i)}, \quad (31)$$

where σ is the corresponding 1σ error. The parameter μ_0 is a nuisance parameter but it is independent of the data points. One can perform an uniform marginalization over μ_0 . However, there is an alternative way. Following [25, 26], the minimization with respect to μ_0 can be made by expanding the χ_μ^2 of Eq. (31) with respect to μ_0 as

$$\chi_\mu^2(\mathbf{p}) = \tilde{A} - 2\mu_0 \tilde{B} + \mu_0^2 \tilde{C}, \quad (32)$$

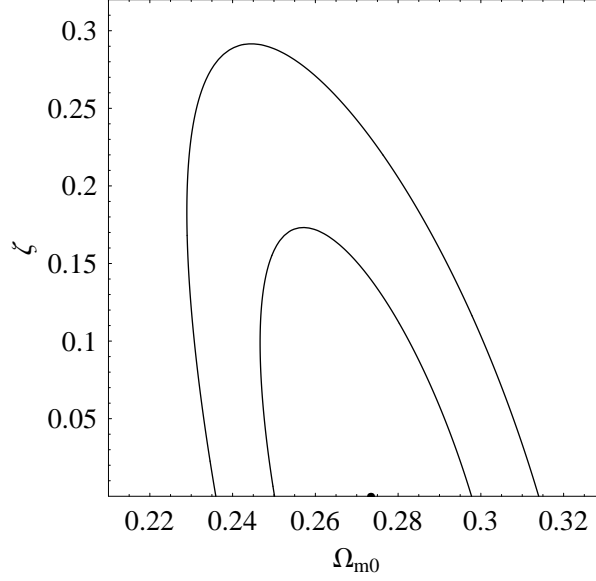


FIG. 2: The same as in Fig. 1, except that this result is obtained by using the combined observational data of 557 Union2 SNIa and the distance parameter A from LSS.

where

$$\tilde{A}(\mathbf{p}) = \sum_i \frac{[\mu_{obs}(z_i) - \mu_{th}(z_i; \mu_0 = 0, \mathbf{p})]^2}{\sigma_{\mu_{obs}}^2(z_i)},$$

$$\tilde{B}(\mathbf{p}) = \sum_i \frac{\mu_{obs}(z_i) - \mu_{th}(z_i; \mu_0 = 0, \mathbf{p})}{\sigma_{\mu_{obs}}^2(z_i)}, \quad \tilde{C} = \sum_i \frac{1}{\sigma_{\mu_{obs}}^2(z_i)}.$$

Eq. (32) has a minimum for $\mu_0 = \tilde{B}/\tilde{C}$ at

$$\tilde{\chi}_\mu^2(\mathbf{p}) = \tilde{A}(\mathbf{p}) - \frac{\tilde{B}(\mathbf{p})^2}{\tilde{C}}. \quad (33)$$

Since $\chi_{\mu, min}^2 = \tilde{\chi}_{\mu, min}^2$ obviously, we can instead minimize $\tilde{\chi}_\mu^2$ which is independent of μ_0 . The best-fit model parameters are determined by minimizing the total χ^2 . When SNIa is used alone, we have $\chi^2 = \tilde{\chi}_\mu^2$ which is given in Eq. (33). As in [27, 28], the 68.3% confidence level is determined by $\Delta\chi^2 \equiv \chi^2 - \chi_{min}^2 \leq 1.0, 2.3$ and 3.53 for $n_p = 1, 2$ and 3 , respectively, where n_p is the number of free model parameters. Similarly, the 95.4% confidence level is determined by $\Delta\chi^2 \equiv \chi^2 - \chi_{min}^2 \leq 4.0, 6.17$ and 8.02 for $n_p = 1, 2$ and 3 , respectively. In the MEF model, there are 2 free model parameters, namely Ω_{m0} and ζ . Note that $E(z)$ for the MEF model has been given in Eq. (28). By minimizing the corresponding χ^2 , we find the best-fit parameters $\Omega_{m0} = 0.2704$ and $\zeta = 4 \times 10^{-7}$, while $\chi_{min}^2 = 542.683$. In Fig. 1, we present the corresponding 68.3% and 95.4% confidence level contours in the $\Omega_{m0} - \zeta$ parameter space.

Next, we add the data from the observation of the large-scale structure (LSS). Here we use the distance parameter A of the measurement of the baryon acoustic oscillation (BAO) peak in the distribution of SDSS luminous red galaxies [29, 30], which contains the main information of the observations of LSS. The distance parameter A is given by

$$A \equiv \Omega_{m0}^{1/2} E(z_b)^{-1/3} \left[\frac{1}{z_b} \int_0^{z_b} \frac{d\tilde{z}}{E(\tilde{z})} \right]^{2/3}, \quad (34)$$

where $z_b = 0.35$. In [30], the value of A has been determined to be $0.469 (n_s/0.98)^{-0.35} \pm 0.017$. Here the scalar spectral index n_s is taken to be 0.963, which has been updated from the WMAP 7-year (WMAP7) data [31]. Now, the total $\chi^2 = \tilde{\chi}_\mu^2 + \chi_{LSS}^2$, where $\tilde{\chi}_\mu^2$ is given in Eq. (33), and $\chi_{LSS}^2 = (A - A_{obs})^2 / \sigma_A^2$. By minimizing the corresponding χ^2 , we find the best-fit parameters $\Omega_{m0} = 0.2733$ and $\zeta = 9 \times 10^{-8}$, while $\chi_{min}^2 = 542.734$. In Fig. 2, we present the corresponding 68.3% and 95.4% confidence level contours in the $\Omega_{m0} - \zeta$ parameter space. Comparing Fig. 2 with Fig. 1, it is easy to see that the constraints become much tighter.

Then, we further add the data from the observation of the cosmic microwave background (CMB). Here we use the the shift parameter R , which contains the main information of the observations of the CMB [31–33]. The shift parameter R of the CMB is defined by [32, 33]

$$R \equiv \Omega_{m0}^{1/2} \int_0^{z_*} \frac{d\tilde{z}}{E(\tilde{z})}, \quad (35)$$

where the redshift of recombination $z_* = 1091.3$ which has been updated in the WMAP7 data [31]. The shift parameter R relates the angular diameter distance to the last scattering surface, the comoving size of the sound horizon at z_* and the angular scale of the first acoustic peak in CMB power spectrum of temperature fluctuations [32, 33]. The value of R has been updated to 1.725 ± 0.018 from the WMAP7 data [31]. Now, the total $\chi^2 = \tilde{\chi}_\mu^2 + \chi_{LSS}^2 + \chi_{CMB}^2$, where $\chi_{CMB}^2 = (R - R_{obs})^2 / \sigma_R^2$. By minimizing the corresponding χ^2 , we find the best-fit parameters $\Omega_{m0} = 0.2699$ and $\zeta = 0.0165$, while $\chi_{min}^2 = 542.879$. In Fig. 3, we present the corresponding 68.3% and 95.4% confidence level contours in the $\Omega_{m0} - \zeta$ parameter space. Clearly, the constraints become tighter, and the best-fit ζ significantly deviates from zero.

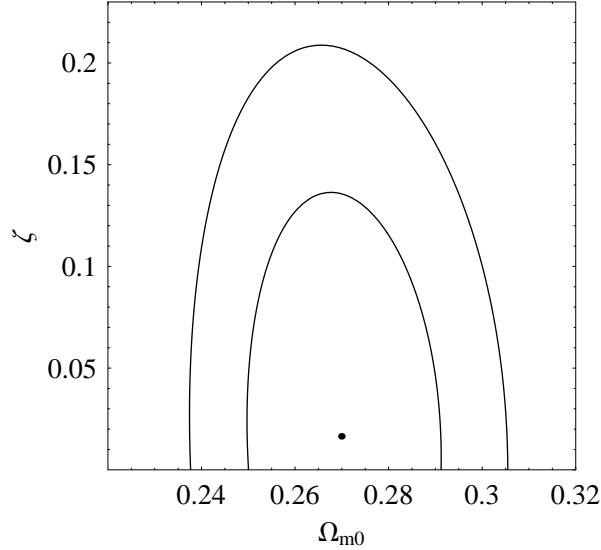


FIG. 3: The same as in Fig. 1, except that this result is obtained by using the combined observational data of 557 Union2 SNIa, the distance parameter A from LSS, and the shift parameter R from CMB.

Finally, we add the 59 Hymnium Gamma-Ray Bursts (GRBs) [28], which can be used to constrain cosmological models without the circularity problem. In fact, GRBs are a complementary probe to SNIa (see e.g. [34] and references therein), whose data points are also given in terms of the distance modulus $\mu_{obs}(z_i)$, similar to the case of SNIa. Therefore, the corresponding χ_{GRB}^2 from 59 Hymnium GRBs is also given in the same form of Eq. (33), but the data points are replaced by the ones of GRBs. Now, the total $\chi^2 = \tilde{\chi}_\mu^2 + \chi_{LSS}^2 + \chi_{CMB}^2 + \chi_{GRB}^2$. By minimizing the corresponding χ^2 , we find the best-fit parameters $\Omega_{m0} = 0.2704$ and $\zeta = 0.0188$, while $\chi_{min}^2 = 566.12$. Note that the number of the total data

points increased by 59, this χ^2_{min} is still very good. In Fig. 4, we present the corresponding 68.3% and 95.4% confidence level contours in the $\Omega_{m0} - \zeta$ parameter space. The difference between Figs. 4 and 3 is small, mainly due to the relatively weak constraint ability of current GRBs sample. This situation will be changed when more and more high-quality GRBs are available in the future.

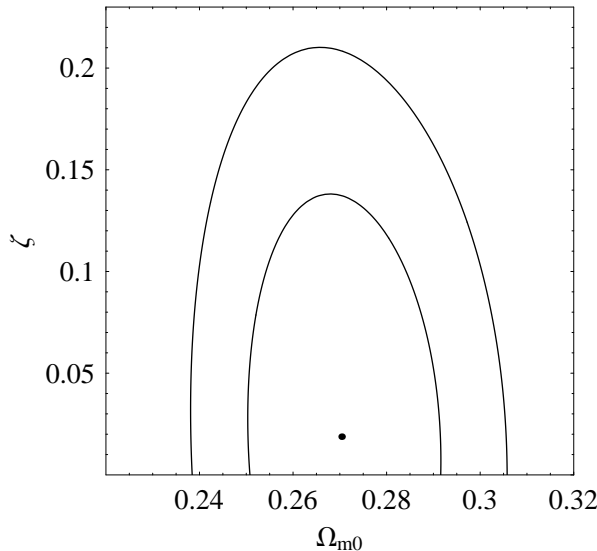


FIG. 4: The same as in Fig. 1, except that this result is obtained by using the combined observational data of 557 Union2 SNIa, the distance parameter A from LSS, the shift parameter R from CMB, and 59 Hymnium GRBs.

III. FURTHER DISCUSSIONS

In the previous section, we have obtained the cosmological constraints on the MEF model. Here, we would like to continue with further discussions.

One of the important issues is to justify the approximate solution $E(z)$ given in Eq. (28). For the very small ζ , such as the $\zeta = 10^{-5}$ in [20] or even smaller, we can of course safely use the approximate solution $E(z)$ given in Eq. (28). The question is when ζ is not so small, can we still safely use the approximate solution $E(z)$ given in Eq. (28)? As the first example, we consider $\zeta = 0.017$ and $\Omega_{m0} = 0.27$, which is near to the best fits of the joint constraints from SNIa+LSS+CMB and SNIa+LSS+CMB+GRBs. We can numerically solve the exact differential equation (23) to find the exact solution of $E(z)$ (of course, the initial condition is $E(z=0) = 1$). To avoid confusion, we label the exact solution from Eq. (23) and the approximate solution $E(z)$ given in Eq. (28) as E_{ex} and E_{app} , respectively. In Fig. 5, we show the difference $\Delta E = E_{app} - E_{ex}$ and the relative difference $\Delta E/E = (E_{app} - E_{ex})/E_{ex}$ for the case with $\zeta = 0.017$ and $\Omega_{m0} = 0.27$. Clearly, the difference between E_{app} and E_{ex} is very small, and hence we can reliably use the approximate solution $E(z)$ given in Eq. (28). Next, we consider a larger ζ . From Figs. 3 and 4, one can see that the upper edges of the 95.4% confidence level contours of the joint constraints from SNIa+LSS+CMB and SNIa+LSS+CMB+GRBs extend to $\zeta \sim 0.2$. So, we choose the case with $\zeta = 0.2$ and $\Omega_{m0} = 0.27$ to be the second example. Again, we present the corresponding ΔE and $\Delta E/E$ in Fig. 6. One can see that the difference between E_{app} and E_{ex} is still fairly small, and hence we can also reliably use the approximate solution $E(z)$ given in Eq. (28). Of course, if the computational ability of the computer becomes more powerful, it is undoubtedly the best choice to use the exact solution E_{ex} from numerically solving Eq. (23). When we work with a less powerful computer, it is suitable to use the approximate solution $E(z)$ given in Eq. (28).

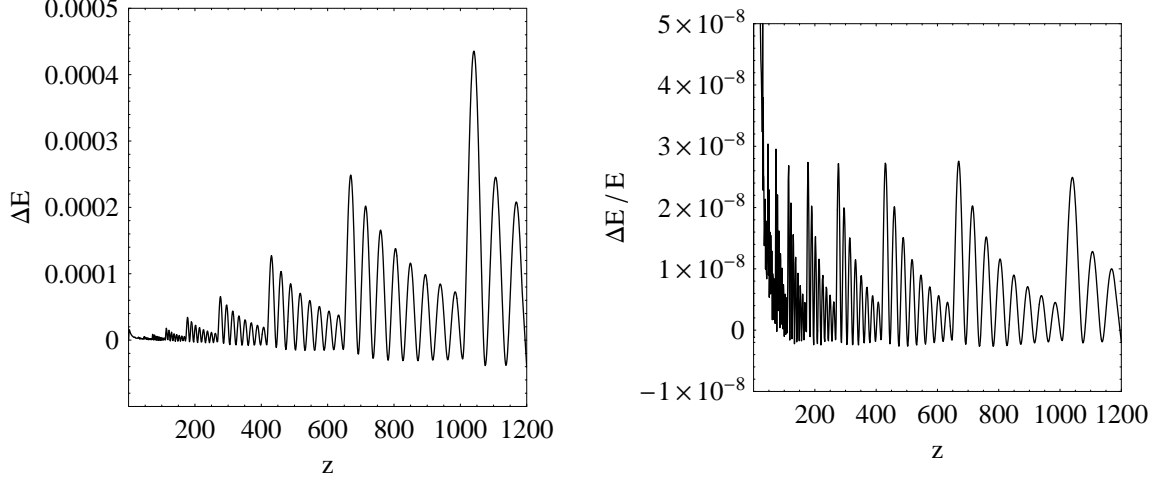


FIG. 5: The difference $\Delta E = E_{app} - E_{ex}$ and the relative difference $\Delta E/E = (E_{app} - E_{ex})/E_{ex}$ for the case with $\zeta = 0.017$ and $\Omega_{m0} = 0.27$. See the text for details.

Next, we turn to the second issue. Although in the text below Eq. (28) we have shown the key point to understand the reason for accelerating the universe without dark energy in the MEF model, it is still desirable to show the visualized plots. As is well known, the deceleration parameter is given by [35]

$$q \equiv -\frac{\ddot{a}}{aH^2} = -1 - \frac{\dot{H}}{H^2} = -1 + (1+z)E^{-1}\frac{dE}{dz}. \quad (36)$$

In Fig. 7, we plot the reduced Hubble parameter $E(z)$ given in Eq. (28) and the corresponding deceleration parameter $q(z)$ for the cases with the best-fit parameters of the joint constraints from SNIa+LSS+CMB (black solid lines) and SNIa+LSS+CMB+GRBs (red dashed lines). In fact, the plot lines for both cases of SNIa+LSS+CMB and SNIa+LSS+CMB+GRBs are heavily overlapped. From Fig. 7, we can clearly see that the deceleration parameter q crosses the transition line $q = 0$ at redshift $z_t = 0.75$, and the universe can really be accelerated in the late time without dark energy. By the way, we note that the usual relation

$$w_{\text{eff}} = -1 + \frac{2}{3}(1+z)E^{-1}\frac{dE}{dz} = \frac{1}{3}(2q-1)$$

does not hold in the MEF model, due to the fact that Friedmann equations have been modified. On the contrary, $q(z)$ given in Eq. (36) holds in any models since it comes from definition directly.

Finally, as mentioned in Sec. I, the argument that MEF can avoid the conflict with the experiments testing the inverse square law relies on a small g_D . We know that $g_D = H_D = \zeta H_0$. In [20], Gao chose a tiny $\zeta = 10^{-5}$ for example, which can of course make a very small g_D . However, as shown in this work, the allowed ζ can be in the range $0 \leq \zeta \lesssim 0.2$ within 95.4% confidence level. Notice that the strength of gravitational fields are of order $10 \text{ N} \cdot \text{kg}^{-1}$ on the Earth, $10^{-4} \text{ N} \cdot \text{kg}^{-1}$ in the solar system [20]. For the best-fit $\zeta \sim 10^{-2}$, the corresponding $g_D = H_D = \zeta H_0 \sim 10^{-12} \text{ N} \cdot \text{kg}^{-1}$. Even for the upper bound $\zeta \sim 10^{-1}$, the corresponding $g_D = H_D = \zeta H_0 \sim 10^{-11} \text{ N} \cdot \text{kg}^{-1}$. Therefore, on the Earth or in the solar system, $g \gg g_D$, hence $x = g_D/g \ll 1$, and then we have $D(x) \rightarrow 1$. Since the experiments testing the inverse square law were done on the Earth or in the solar system, the deviation from the inverse square law are extremely tiny. The significant deviation from the inverse square law can only occur in the very large scale in the universe where the gravitational fields are very weak, and hence it can escape the detection of the experiments testing the inverse square law which were done on the Earth or in the solar system.

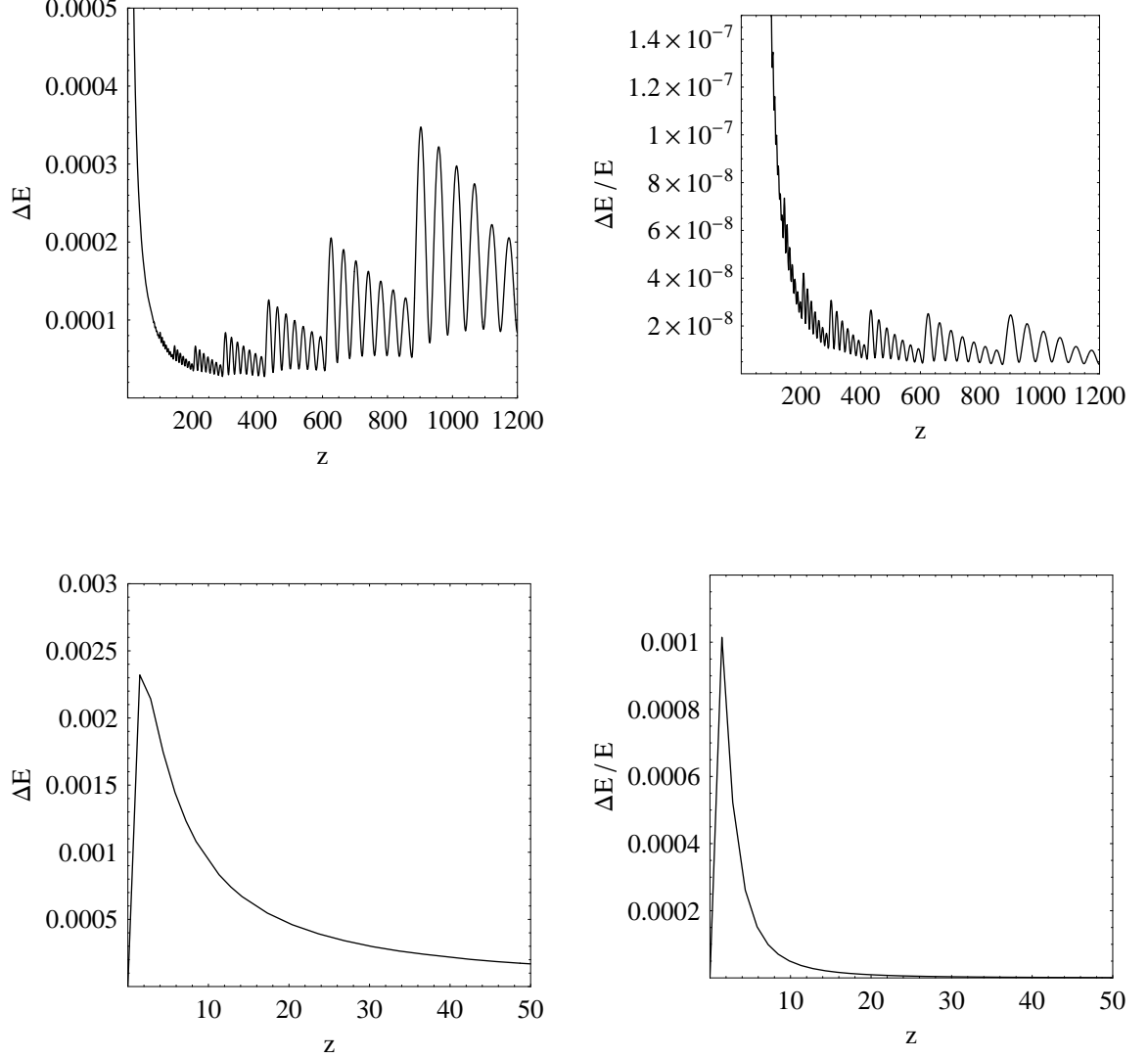


FIG. 6: The same as in Fig. 5, except for the case with $\zeta = 0.2$ and $\Omega_{m0} = 0.27$. The bottom panels are the enlarged parts in the redshift range $0 \leq z \leq 50$.

IV. CONCLUSION AND REMARKS

In summary, we considered the cosmological constraints on the MEF model in this work, by using the observational data of 557 Union2 SNIa, the distance parameter A from LSS, the shift parameter R from CMB, and 59 Hymnium GRBs. We found that the key parameter ζ in MEF model has been limited in a narrow range $0 \leq \zeta \lesssim 0.2$ within 95.4% confidence level. By using the important result given in Eq. (28), we have clearly shown the key point to understand the reason for accelerating the universe without dark energy in the MEF model. We showed the MEF model reduces to Λ CDM model when $\zeta \ll 1$. However, the best-fit ζ for the observations SNIa+LSS+CMB and SNIa+LSS+CMB+GRBs significantly deviates from zero. This indicates the new feature of MEF model different from Λ CDM model. We have justified

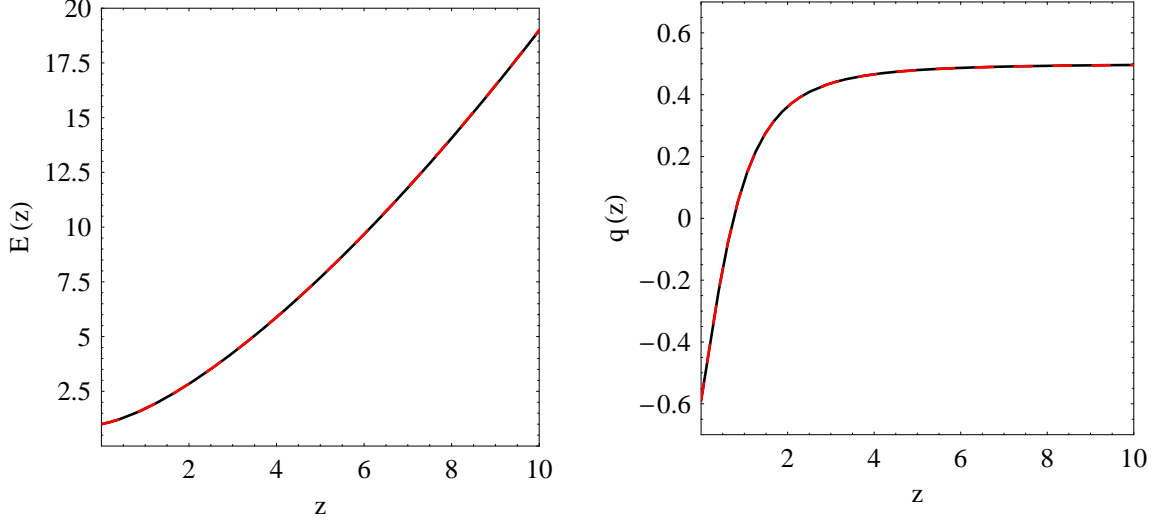


FIG. 7: The reduced Hubble parameter $E(z)$ given in Eq. (28) and the corresponding deceleration parameter $q(z)$ for the cases with the best-fit parameters of the joint constraints from SNIa+LSS+CMB (black solid lines) and SNIa+LSS+CMB+GRBs (red dashed lines).

the approximate solution $E(z)$ given in Eq. (28). We plotted $E(z)$ and $q(z)$ as functions of redshift z , and clearly showed that the universe can be accelerated in late time without dark energy. Finally, we have shown that MEF can avoid the conflict with the experiments testing the inverse square law.

After all, some remarks are in order. In the MEF model, as shown in this work, the universe can be accelerated without dark energy. The only component is dust matter. The MEF model is in fact a modified gravity model, similar to the $f(R)$ models and the braneworld models. The MEF model can be degenerate to Λ CDM model, but it has not an explicit cosmological constant in the model. This is a big advantage in fact, beyond some $f(R)$ and braneworld models in this sense.

Secondly, we point out the possibility to extend the original MEF model. In principle, it is not necessary to restrict the energy component in the universe to be dust matter only. The universe can contain other components, such as, dark energy. For example, we can consider a universe containing both dust matter and dark energy whose equation-of-state parameter (EoS) w_X is a constant. In this case, the total energy density $\rho = \rho_m + \rho_X = \rho_{m0} a^{-3} + \rho_{X0} a^{-3(1+w_X)}$. Substituting into Eq. (20), we have

$$\left[-2D \left(\frac{\zeta}{E} \right) + \frac{3\zeta/E}{e^{\zeta/E} - 1} \right] \cdot 2E \frac{dE}{dz} = 3\Omega_{m0} (1+z)^2 + 3(1+w_X) \Omega_{X0} (1+z)^{3w_X+2}, \quad (37)$$

where $\Omega_{X0} \equiv (8\pi G \rho_{X0}) / (3H_0^2)$. Note that $\Omega_{m0} + \Omega_{X0} \neq 1$, since Friedmann equation has been modified in the MEF model. In principle, one can numerically solve Eq. (37) to get $E(z)$. Similar to the original MEF model, we find that an approximation of the exact differential equation (37) is given by

$$\left(1 - \frac{3}{4} \frac{\zeta}{E} \right) \cdot 2E dE = \Omega_{m0} da^{-3} + \Omega_{X0} da^{-3(1+w_X)}. \quad (38)$$

Integrating Eq. (38), we have

$$E^2 - \frac{3}{2} \zeta E = \Omega_{m0} a^{-3} + \Omega_{X0} a^{-3(1+w_X)} + \text{const.}, \quad (39)$$

where *const.* is the integral constant, which can be determined by requiring $E(z=0) = 1$. Finally, we find that

$$E^2 - \frac{3}{2} \zeta E = \Omega_{m0} (1+z)^3 + \Omega_{X0} (1+z)^{3(1+w_X)} + \left(1 - \frac{3}{2} \zeta - \Omega_{m0} - \Omega_{X0} \right), \quad (40)$$

which is a quadratic equation of E in fact. Noting that E is positive, we solve Eq. (40) to get

$$E(z) = \frac{3}{4}\zeta + \frac{1}{2} \left\{ \frac{9}{4}\zeta^2 + 4 \left[\Omega_{m0}(1+z)^3 + \Omega_{X0}(1+z)^{3(1+w_X)} + \left(1 - \frac{3}{2}\zeta - \Omega_{m0} - \Omega_{X0} \right) \right] \right\}^{1/2}. \quad (41)$$

In fact, this is just a simple example. One can include any type of dark energy, for instance, the CPL dark energy whose EoS is given by $w_{de} = w_0 + w_a(1-a)$, quintessence, phantom, k-essence, hessence, (generalized) Chaplygin gas, holographic/agegraphic dark energy, vector-like dark energy, spinor dark energy, and so on. Therefore, we would like to give the more general formulae. In this case, the total energy density $\rho = \rho_m + \rho_{de} = \rho_{m0} a^{-3} + \rho_{de,0} f(a)$, where $f(a)$ can be any function of a which satisfies $f(a=1) = 1$. Substituting into Eq. (20), we obtain

$$\left[-2D \left(\frac{\zeta}{E} \right) + \frac{3\zeta/E}{e^{\zeta/E} - 1} \right] \cdot 2E \frac{dE}{dz} = 3\Omega_{m0}(1+z)^2 - \Omega_{de,0}(1+z)^{-2} f', \quad (42)$$

where $f' \equiv df/da$, and $\Omega_{de,0} \equiv (8\pi G \rho_{de,0})/(3H_0^2)$. Note again that $\Omega_{m0} + \Omega_{de,0} \neq 1$, since Friedmann equation has been modified in the MEF model. Eq. (42) is the exact differential equation, which can be used to find the exact $E(z)$ numerically. Also, we give the corresponding approximate solution as

$$E(z) = \frac{3}{4}\zeta + \frac{1}{2} \left\{ \frac{9}{4}\zeta^2 + 4 \left[\Omega_{m0}(1+z)^3 + \Omega_{de,0} f \left(\frac{1}{1+z} \right) + \left(1 - \frac{3}{2}\zeta - \Omega_{m0} - \Omega_{de,0} \right) \right] \right\}^{1/2}. \quad (43)$$

Similarly, if one need to add other component, such as radiation, it is not a hard work. In fact, we can give the most general formulae. In this case, the total energy density $\rho = \rho_0 f(a)$, where $f(a)$ can be any function of a which satisfies $f(a=1) = 1$. Substituting into Eq. (20), we have

$$\left[-2D \left(\frac{\zeta}{E} \right) + \frac{3\zeta/E}{e^{\zeta/E} - 1} \right] \cdot 2E \frac{dE}{dz} = -\Omega_0(1+z)^{-2} f', \quad (44)$$

where $\Omega_0 \equiv (8\pi G \rho_0)/(3H_0^2)$. Note again that $\Omega_0 \neq 1$, since Friedmann equation has been modified in the MEF model, namely $H^2 \neq (8\pi G \rho)/3$. Eq. (44) is the exact differential equation, which can be used to find the exact $E(z)$ numerically. Also, we give the corresponding approximate solution as

$$E(z) = \frac{3}{4}\zeta + \frac{1}{2} \left\{ \frac{9}{4}\zeta^2 + 4 \left[\Omega_0 f \left(\frac{1}{1+z} \right) + \left(1 - \frac{3}{2}\zeta - \Omega_0 \right) \right] \right\}^{1/2}. \quad (45)$$

In fact, noting that $E = H/H_0$, Eq. (45) can be regarded as the approximate modified Friedmann equation in the MEF model. If $\zeta \ll 1$, Eq. (45) reduces to

$$H^2 = \frac{8\pi G}{3} \rho + \Lambda_{\text{eff}}, \quad (46)$$

where $\Lambda_{\text{eff}} = (1 - \Omega_0) H_0^2 = \text{const.}$ is actually an effective cosmological constant. Therefore, in the most general case, we can clearly reveal the implicit root to accelerate the universe in the MEF model, regardless of the energy components in the universe. An effective cosmological constant is the intrinsic feature (we refer to e.g. [23] for a previous insight). The other exotic features of the MEF model could emerge only when ζ significantly deviates from zero.

Thirdly, we would like to say some words on the understanding of the original entropic force model [1] and the modified entropic force model [20]. In fact, entropic force is just a new perspective to gravity, from the thermodynamical point of view. So, the original entropic force can only recover all results of the usual (Newton and Einstein) gravity. The only new thing is the reversed logic which might reveal the nature of gravity. In the original entropic force model [1], using the fundamental assumptions Eqs. (1), (3), (5) and (6), Verlinde derived the Newton's law of gravitation Eq. (8) for the (non-relativistic) Euclidean spacetime in section 3 of [1], and also derived the Einstein gravitational equations for any (relativistic) curved spacetime in section 5 of [1]. On the other hand, the Friedmann equations were derived in [5, 6] for the Friedmann-Robertson-Walker (FRW) universe. There is *no* any mixing here. We should mention

that both the original entropic force [1] and the modified entropic force [20] cannot be understood in *only* non-relativistic or relativistic cases. In fact, they are equivalent to gravity itself in all cases. As the usual understanding, the Newton's law of gravitation is just the approximation of Einstein gravitational equations in the (non-relativistic) small scale limit, whereas the Friedmann equations are just the special case of Einstein gravitational equations in the cosmic scale (homogeneous and isotropic spacetime). The situation is similar in the modified entropic force model. Using the fundamental assumptions Eqs. (1), (3), (5) and (11), in [20] Gao derived the Newton's law of gravitation Eq. (14) for the (non-relativistic) Euclidean spacetime, and also derived the second Friedmann equation (16) for the FRW universe. Note that the first Friedmann equation can be derived from the second Friedmann equation (16) and the energy conservation equation (19). On the other hand, following Verlinde's derivations in section 5 of [1], one can derive the corresponding (modified) Einstein gravitational equations for any (relativistic) curved spacetime. In fact, this is just the lacked sector in the modified entropic force model. However, it is available in principle, although it has not been given in the literature. In the modified entropic force model, there is *no* any mixing too. The modified Newton's law of gravitation Eq. (14) is just the approximation of the (lacked but available in principle) modified Einstein gravitational equations in the (non-relativistic) small scale limit, whereas the modified second Friedmann equation (16) is just the special case of the (lacked but available in principle) modified Einstein gravitational equations in the cosmic scale (homogeneous and isotropic spacetime).

Fourthly, we said that the MEF model is similar to $f(R)$ -gravity or braneworld scenario. Notice that they are similar *only* in the sense that the gravity has been modified in these models. Of course, both $f(R)$ -gravity and braneworld scenario were derived from the known actions, whereas the action for MEF is still lacked in the literature. However, as mentioned above, following Verlinde's derivations in section 5 of [1], in principle one can derive the corresponding (modified) Einstein gravitational equations for any (relativistic) curved spacetime. Once this lacked sector has been done, the explicit action is ready. Since the present work focuses on cosmology in the MEF model, we leave this task to future works.

Fifthly, as mentioned in this work, in the MEF model, there is *no* dark energy in fact. The universe is matter-dominated always. The expansion of our universe is accelerated due to the fact that gravity has been modified. In the non-relativistic case, there is no dark energy too, but gravity is also modified. However, as mentioned in this work, this modification to Newtonian gravity is negligible on the Earth or in the solar system. In the larger scale, the modified gravity is described by Eq. (14). As shown in [37], the Debye entropic force can be an alternative to the modified Newtonian dynamics (MOND) to explain the rotational velocity curves of spiral galaxies. In fact, the MEF model [20] and the Debye entropic force model [37] are very similar. So, it is anticipated that the "non-relativistic cosmology" of the MEF model could be an alternative to dark matter, which is usually invoked to explain the rotational velocity curves of spiral galaxies.

Finally, we admit that the entropic force proposed by Verlinde is based on several unproved hypotheses, and it is still controversial in the physical community. On the other hand, the Debye model in the thermodynamics has not been used in the gravity theory previously. However, in the history, many great theories also appeared controversially in their beginning. Therefore, we consider that it is better to keep an open mind to these speculative attempts.

ACKNOWLEDGEMENTS

We thank the anonymous referee for quite useful comments and suggestions, which help us to improve this work. We are grateful to Professors Rong-Gen Cai, Shuang Nan Zhang and Miao Li for helpful discussions. We also thank Minzi Feng, as well as Xiao-Peng Ma and Bo Tang, for kind help and discussions. This work was supported in part by NSFC under Grant No. 10905005, the Excellent Young Scholars Research Fund of Beijing Institute of Technology, and the Fundamental Research Fund of Beijing Institute of Technology.

[1] E. P. Verlinde, arXiv:1001.0785 [hep-th].

- [2] T. Jacobson, Phys. Rev. Lett. **75**, 1260 (1995) [gr-qc/9504004].
- [3] T. Padmanabhan, Mod. Phys. Lett. A **25**, 1129 (2010) [arXiv:0912.3165].
- [4] J. D. Bekenstein, Phys. Rev. D **7**, 2333 (1973).
- [5] R. G. Cai, L. M. Cao and N. Ohta, Phys. Rev. D **81**, 061501 (2010) [arXiv:1001.3470].
- [6] F. W. Shu and Y. G. Gong, arXiv:1001.3237 [gr-qc].
- [7] L. Smolin, arXiv:1001.3668 [gr-qc].
- [8] M. Li and Y. Wang, Phys. Lett. B **687**, 243 (2010) [arXiv:1001.4466].
- [9] D. A. Easson, P. H. Frampton and G. F. Smoot, arXiv:1002.4278 [hep-th];
D. A. Easson, P. H. Frampton and G. F. Smoot, arXiv:1003.1528 [hep-th].
- [10] Y. Tian and X. Wu, Phys. Rev. D **81**, 104013 (2010) [arXiv:1002.1275].
- [11] Y. S. Myung, arXiv:1002.0871 [hep-th].
- [12] I. V. Vanea and M. A. Santos, arXiv:1002.2454 [hep-th].
- [13] Y. Zhang, Y. G. Gong and Z. H. Zhu, arXiv:1001.4677 [hep-th].
- [14] A. Sheykhi, Phys. Rev. D **81**, 104011 (2010) [arXiv:1004.0627].
- [15] L. Modesto and A. Randono, arXiv:1003.1998 [hep-th].
- [16] Y. F. Cai, J. Liu and H. Li, Phys. Lett. B **690**, 213 (2010) [arXiv:1003.4526].
- [17] Y. Wang, arXiv:1001.4786 [hep-th];
T. Wang, Phys. Rev. D **81**, 104045 (2010) [arXiv:1001.4965];
Y. Ling and J. P. Wu, arXiv:1001.5324 [hep-th];
L. Zhao, arXiv:1002.0488 [hep-th];
Y. X. Liu, Y. Q. Wang and S. W. Wei, arXiv:1002.1062 [hep-th];
R. G. Cai, L. M. Cao and N. Ohta, Phys. Rev. D **81**, 084012 (2010) [arXiv:1002.1136];
X. Kuang, Y. Ling and H. Zhang, arXiv:1003.0195 [gr-qc];
X. G. He and B. Q. Ma, Chin. Phys. Lett. **27**, 070402 (2010) [arXiv:1003.1625];
Q. Pan and B. Wang, arXiv:1004.2954 [hep-th].
- [18] J. Kowalski-Glikman, Phys. Rev. D **81**, 084038 (2010) [arXiv:1002.1035];
R. A. Konoplya, arXiv:1002.2818 [hep-th];
S. Ghosh, arXiv:1003.0285 [hep-th];
C. J. Hogan, arXiv:1002.4880 [gr-qc];
U. H. Danielsson, arXiv:1003.0668 [hep-th];
J. Munkhammar, arXiv:1003.1262 [hep-th];
R. Banerjee and B. R. Majhi, arXiv:1003.2312 [gr-qc];
S. Samanta, arXiv:1003.5965 [hep-th];
A. Morozov, arXiv:1003.4276 [hep-th];
R. Casadio and A. Gruppiso, arXiv:1005.0790 [gr-qc].
- [19] Y. S. Myung and Y. W. Kim, Phys. Rev. D **81**, 105012 (2010) [arXiv:1002.2292];
J. W. Lee, H. C. Kim and J. Lee, arXiv:1001.5445 [hep-th];
J. Makea, arXiv:1001.3808 [gr-qc];
E. Chang-Young, M. Eune, K. Kimm and D. Lee, arXiv:1003.2049 [gr-qc];
Y. S. Myung, arXiv:1003.5037 [hep-th];
J. W. Lee, arXiv:1003.4464 [hep-th];
J. W. Lee, arXiv:1003.1878 [hep-th].
- [20] C. J. Gao, Phys. Rev. D **81**, 087306 (2010) [arXiv:1001.4585].
- [21] D. V. Schroeder, *An Introduction to Thermal Physics*, Addison-Wesley, San Francisco, California (2000).
- [22] See, for instance, the entry of Debye model in Wikipedia at http://en.wikipedia.org/wiki/Debye_model
- [23] R. G. Cai and S. P. Kim, JHEP **0502**, 050 (2005) [hep-th/0501055];
R. G. Cai, L. M. Cao and Y. P. Hu, Class. Quant. Grav. **26**, 155018 (2009) [arXiv:0809.1554].
- [24] R. Amanullah *et al.* [Supernova Cosmology Project Collaboration], arXiv:1004.1711 [astro-ph.CO].
The numerical data of the full Union2 sample are available at <http://supernova.lbl.gov/Union>
- [25] E. Di Pietro and J. F. Claeskens, Mon. Not. Roy. Astron. Soc. **341**, 1299 (2003) [astro-ph/0207332].
- [26] Y. Wang and P. Mukherjee, Astrophys. J. **650**, 1 (2006) [astro-ph/0604051].
- [27] S. Nesseris and L. Perivolaropoulos, Phys. Rev. D **70**, 043531 (2004) [astro-ph/0401556].
- [28] H. Wei, JCAP **1008**, 020 (2010) [arXiv:1004.4951].
- [29] M. Tegmark *et al.* [SDSS Collaboration], Phys. Rev. D **69**, 103501 (2004) [astro-ph/0310723];
M. Tegmark *et al.* [SDSS Collaboration], Astrophys. J. **606**, 702 (2004) [astro-ph/0310725];

- U. Seljak *et al.* [SDSS Collaboration], Phys. Rev. D **71**, 103515 (2005) [astro-ph/0407372];
M. Tegmark *et al.* [SDSS Collaboration], Phys. Rev. D **74**, 123507 (2006) [astro-ph/0608632].
- [30] D. J. Eisenstein *et al.* [SDSS Collaboration], Astrophys. J. **633**, 560 (2005) [astro-ph/0501171].
- [31] E. Komatsu *et al.* [WMAP Collaboration], arXiv:1001.4538 [astro-ph.CO].
- [32] Y. Wang and P. Mukherjee, Astrophys. J. **650**, 1 (2006) [astro-ph/0604051].
- [33] J. R. Bond, G. Efstathiou and M. Tegmark, Mon. Not. Roy. Astron. Soc. **291**, L33 (1997) [astro-ph/9702100].
- [34] B. E. Schaefer, Astrophys. J. **660**, 16 (2007) [astro-ph/0612285].
- [35] H. Wei, arXiv:1002.4230 [gr-qc];
H. Wei and S. N. Zhang, Phys. Lett. B **644**, 7 (2007) [astro-ph/0609597].
- [36] F. Caravelli and L. Modesto, arXiv:1001.4364 [gr-qc];
Y. Zhao, arXiv:1002.4039 [hep-th];
P. Mahato, arXiv:1004.1818 [gr-qc].
- [37] X. Li and Z. Chang, arXiv:1005.1169 [hep-th].
- [38] S. Gao, arXiv:1002.2668 [gr-qc].
- [39] H. Culetu, arXiv:1002.3876 [hep-th].
- [40] S. Hossenfelder, arXiv:1003.1015 [gr-qc].
- [41] Y. S. Myung, arXiv:1003.5037 [hep-th];
Y. S. Myung, arXiv:1005.2240 [hep-th].
- [42] M. Li and Y. Pang, Phys. Rev. D **82**, 027501 (2010) [arXiv:1004.0877].
- [43] J. P. Lee, arXiv:1005.1347 [hep-th].